biomolecules

MDPI

Article

Plasma Polyamine Biomarker Panels: Agmatine in Support of Prostate Cancer Diagnosis

Donatella Coradduzza [1], Tatiana Solinas [2], Emanuela Azara [3], Nicola Culeddu [3], Sara Cruciani [1], Angelo Zinellu [1], Serenella Medici [4], Margherita Maioli [1], Massimo Madonia [2] and Ciriaco Carru [1,5,*]

[1] Department of Biomedical Sciences, University of Sassari, 07100 Sassari, Italy; donatella.coradduzza@libero.it (D.C.); sara.cruciani@outlook.com (S.C.); azinellu@uniss.it (A.Z.); mmaioli@uniss.it (M.M.)
[2] Department of Clinical and Experimental Medicine, Urologic Clinic, University of Sassari, 07100 Sassari, Italy; tatiana.solinas@aousassari.it (T.S.); madonia@uniss.it (M.M.)
[3] Institute of Biomolecular Chemistry, National Research Council, 07100 Sassari, Italy; emanuelagigliola.azara@cnr.it (E.A.); nculeddu@icb.cnr.it (N.C.)
[4] Department of Chemistry and Pharmacy, University of Sassari, 07100 Sassari, Italy; sere@uniss.it
[5] Department of Biomedical Sciences and University Hospital of Sassari (AOU), 07100 Sassari, Italy
* Correspondence: carru@uniss.it

Abstract: Prostate cancer is the most frequent malignant tumour among males (19%), often clinically silent and of difficult prognosis. Although several studies have highlighted the diagnostic and prognostic role of circulating biomarkers, such as PSA, their measurement does not necessarily allow the detection of the disease. Within this context, many authors suggest that the evaluation of circulating polyamines could represent a valuable tool, although several analytical problems still counteract their clinical practice. In particular, agmatine seems particularly intriguing, being a potential inhibitor of polyamines commonly derived from arginine. The aim of the present work was to evaluate the potential role of agmatine as a suitable biomarker for the identification of different classes of patients with prostate cancer (PC). For this reason, three groups of human patients—benign prostatic hyperplasia (BPH), precancerous lesion (PL), and prostate cancer (PC)—were recruited from a cohort of patients with suspected prostate cancer (n = 170), and obtained plasma was tested using the LC-HRMS method. Statistics on the receiver operating characteristics curve (ROC), and multivariate analysis were used to examine the predictive value of markers for discrimination among the three patient groups. Statistical analysis models revealed good discrimination using polyamine levels to distinguish the three classes of patients. AUC above 0.8, sensitivity ranging from 67% to 89%, specificity ranging from 74% to 89% and accuracy from 73% to 86%, considering the validation set, were achieved. Agmatine plasma levels were measured in PC (39.9 $\pm$ 12.06 ng/mL), BPH (77.62 $\pm$ 15.05 ng/mL), and PL (53.31 $\pm$ 15.27 ng/mL) patients. ROC analysis of the agmatine panel showed an AUC of 0.959 and $p \leq 0.001$. These results could represent a future tool able to discriminate patients belonging to the three different clinical groups.

Keywords: prostate cancer; biomarkers; agmatine; LC-HRMS

Citation: Coradduzza, D.; Solinas, T.; Azara, E.; Culeddu, N.; Cruciani, S.; Zinellu, A.; Medici, S.; Maioli, M.; Madonia, M.; Carru, C. Plasma Polyamine Biomarker Panels: Agmatine in Support of Prostate Cancer Diagnosis. *Biomolecules* **2022**, *12*, 514. https://doi.org/10.3390/biom12040514

Academic Editor: Alessandro Alaimo

Received: 28 January 2022
Accepted: 26 March 2022
Published: 29 March 2022

1. Introduction

Prostate cancer is the most frequent neoplasm among men, and is the fifth leading cause of death worldwide, with the risk increasing with age [1]. Most cancers arise in the periphery of the prostate gland, and cause symptoms only when they have grown to compress the urethra or invade the sphincter or neurovascular bundle [2]. Early prostate cancer usually does not cause pain, and most affected men exhibit no noticeable symptoms. Within this context, clinical assessment of the onset of this disease is complicated by its clinically silent and biologically non-aggressive form. Severities and outcomes of prostate cancer is differ widely. Early-stage prostate cancer can usually be treated successfully,

while some older men have prostate tumours that grow so slowly, being biologically non-aggressive, that they may never cause health problems during their lifetime. On the other hand, in other men, the cancer is much more aggressive. Some cancerous tumours can invade surrounding tissue and spread to other parts of the body, leading to metastatic cancers. PSA screening is recommended, by the European Society of Medical Oncology (ESMO) after the age of 50 [3]. Screening tests for prostate cancer include digital rectal examination (DRE), prostate-specific antigen (PSA) blood test, trans rectal ultrasound guided (TRUS) biopsy and prostate biopsy, with the latter being considered the gold standard [4]. Screening and regular follow-up, in which PSA determination plays an important role, is an important step in reducing cancer mortality. Nevertheless, there is still a large grey area of patients that have threshold values for this marker, making it confusing for diagnosis [5,6]. Actually, this leads to overdiagnosis, increasing the burden on the health care system with the unnecessary implementation of invasive diagnostic and therapeutic interventions [7]. Serum and plasma tests are less invasive and faster to perform than tissue biopsies, thereby making them more suitable [8]. Recently, diagnostic tests based either on biomarkers found in urine, such as PCA3, T2-ERG, exosome, and others, or in blood, such as four kallikrein proteins, have been studied [5,6,9,10]. Within this context, different authors have proposed a multi-analyte blood test (Cancer-SEEK) for assessing cancer type based on multiple analytes [11,12]. Furthermore, since inflammation seems to play a key role in the evolution of cancer diseases [13], the role of several biomarkers of inflammation [14] derived from blood counts has been investigated: neutrophil/lymphocyte ratio (NLR), NLR derivative (dNLR = neutrophils/(white blood cells-neutrophils)), platelet/lymphocyte ratio (PLR), monocyte/lymphocyte ratio (MLR), (neutrophils × mono-cytes)/lymphocyte ratio (SIRI), and (neutrophils × monocytes × platelets)/lymphocyte ratio (AISI). Many authors consider the role of polyamines belonging to the arginine and lysine cycle to be very relevant among circulating biomarkers, and changes in their plasma concentration have been studied as biomarkers for various cancers.

Polyamines are small aliphatic polycations that bind several negatively charged molecules under physiological conditions, including DNA, RNA, ATP, certain types of proteins, and phospholipids [7,8]. Thus, they play an essential role in cell growth, proliferation, differentiation, development, immunity, migration, gene regulation, DNA stability, and protein and nucleic acid synthesis [4,7,9,10]. Other functions include cell adhesion and extracellular matrix repair, and they are involved in specific signalling processes. Polyamine levels are maintained within a narrow range, leading to severe physiological effects when dysregulated. Indeed, a pronounced decrease in polyamine levels can prevent cell proliferation and migration [9,15]. On the other hand, an excess of polyamines results in apoptosis and cell transformation [9]. In mammalian cells, the parental polyamines are synthesised from ornithine by an initial decarboxylation step to putrescine, catalysed by the enzyme ornithine decarboxylase (ODC) [16]. This step is followed by other enzyme-catalysed aminopropyl transfer reactions via spermidine synthase (SRM) and spermine synthase (SMS), generating spermidine and spermine, respectively [8,9,17].

Recently, in mammalian systems, agmatine was identified as a new polyamine from arginine decarboxylation [18,19].

Agmatine is an important biogenic amine, and could regulate polyamine metabolism [10], playing key roles in cellular metabolism and the inhibition or induction of cell proliferation, depending on its numerous interactions with the tumour environment [20–30]. Polyamines and their metabolites exist in both tissue and physiological fluid; their distribution throughout the body is not the same, especially in carcinogenesis [31,32]. ODC is the restricting enzyme, regulated by androgens in the prostate gland [33], and the gene encoding ODC is markedly induced in human prostate cancer [34]. It is well known that cancer cell metabolism is dependent on arginine, the so-called 'Achilles' heel' of cancer, making it a potential target for cancer treatment [23,35–37]. Researchers and physicians have expressed the need for biomarkers that are able to discriminate patients in the early stages of prostate cancer (PC) from those with benign prostatic hyperplasia (BPH) or precancerous lesions (PL), the clinical evolution

of which is not always predictable. Benign prostatic hyperplasia (BPH)—also called prostate gland enlargement—is a common condition as men get older. Having BPH does not increase a patient's risk for prostate cancer. An enlarged prostate gland can cause uncomfortable urinary symptoms, such as blocking the flow of urine out of the bladder. The PL category includes patients with a histopathological diagnosis of atypical small acinar proliferation (ASAP) and premalignant proliferation of atypical ductal and acinar cells. Prostatic intraepithelial neoplasia (PIN), particularly high-grade PIN (HGPIN), and atypical small acinar proliferation (ASAP) have been identified as being precancerous lesions of the prostate, that is, they function as precursor lesions to prostatic carcinoma. These are categories with increased risk of developing prostate adenocarcinoma. The chance that a patient diagnosed with ASAP will develop cancer is about 40% [38]. The morphological appearance of HGPIN (i.e., tufting, micropapillary, cribriform, flat) is not always correlated with the consequent development of the neoplasm, meaning that clinical follow-up is highly recommended [39–48]. PIN refers to the precancerous end of a morphologic spectrum involving cellular proliferation within prostatic ducts, ductules, and acini. HGPIN possesses high predictive value for the future development of adenocarcinoma [49], and ASAP has potential significance for the development of synchronic malignant disease close to the source of origin of the biopsy [50]. Both are of great clinical importance for the early diagnosis of PCa. Whether or not the extent of high-grade PIN in biopsies is a predictor of prostate cancer is still controversial [51].

The aim of the present study was to investigate the levels of circulating polyamines in a population of subjects with suspected prostate cancer in order to understand whether they are capable of differentiation among different patient groups and could thus be used for clinical decision support.

To achieve this goal, high-resolution mass spectrometry (HRMS) was used in combination with high-performance liquid chromatography (HPLC), both of which are highly convenient due to their extraction of target ions from the total ion chromatogram, meaning that even minor polyamines can be detected and quantitatively analysed in complex matrices [52].

2. Materials and Methods

2.1. Chemicals and Methods

The reference standards of putrescine, cadaverine hydrochloride, spermidine hydrochloride, spermine, agmatine sulphate salt, *N*-acetyl-putrescine hydrochloride, *N*-acetylspermine trihydrochloride, *N*-acetylspermidine dihydrochloride, l-ornithine hydrochloride, lysine, l-arginine, aminobutyric acid, deuterated histamine, heptafluorobutyric acid (HFBA) and methanol were purchased from Sigma-Aldrich (St. Louis, MO, USA) for analytical type analysis. Water for LCMS was purchased from Fisher Scientific (Fair Lawn, NJ, USA).

Liquid chromatography–high-resolution mass spectrometry (LC-HRMS) analysis was performed using an UPLC Ultimate 3000 (Thermo Fisher-Dionex San Jose, CA, USA) system equipped with a HESI-II electrospray source to a Q-Exactive-Orbitrap™-based mass spectrometer (all from Thermo Scientific, San Jose, CA, USA). Chromatographic separation was carried out on the C18 column of the Gemini C18 (Phenomenex, Torrance, CA, USA), 100 mm × 2 mm, particle size 3 µm, the column was held at 37 °C. Chromatographic separation was achieved with gradient elution using a mobile phase composed of 0.05% heptafluorobutyric acid (HFBA) in water (A) and 0.05% HFBA in methanol (B).

2.2. Plasma Prostate Cancer Sample Preparation

A total of 170 male patients were recruited at the Urology Department of the University Hospital of Sassari between September 2018 and September 2019. The studies were conducted in accordance with the Declaration of Helsinki. Written informed consent was obtained from each subject before the study. Following the clinical diagnosis criteria (TRUS, PB, and biopsy analysis), three subsets of patients were ordered; 92 patients had prostate cancer diagnosed (PC), 50 had benign prostatic hypertrophy or no evidence of malignancy

(BPH), and the remaining 28 had precancerous lesion (PL). Table 1 shows detailed information on demographic, pathological and treatment patients list of the clinical patient's characteristics. All plasma samples were stored at −80 °C for one month between collection and measurement. An aliquot of 250 µL of plasma was transferred into an Eppendorf microtube and mixed with 150 µL of methanol (containing 0.05% HFBA) and 100 µL of water for 50 s. After precipitation, samples were centrifuged for 9 min at 15,000 rpm, and frozen overnight at −20 °C. The supernatant was evaporated to dryness at 36 °C under a stream of nitrogen. The residue was reconstituted into 500 µL of mobile phases and 50 µL of IS (internal standard, deuterated histamine). An aliquot of 5 µL of the solution was injected into the LC-HMRS system for analysis. Plasma sample preparation was performed in the same manner as the quality control (QC) samples. The supernatants obtained from these solutions were also used as the QC samples. The QC sample was a mixture of all samples, containing all information in the plasma samples, and it was used to optimise and supervise the injection process. QC samples were injected occasionally to test the stability of both the samples and the system during acquisition. Prior to sample analysis, the QC samples were injected six times to monitor the stability of the instrument. The six QC samples were then processed in parallel and injected to assess the repeatability of the method.

Table 1. List of characteristics from the clinical records of the patients. * PC vs. PL, ** PC vs. BPH. N.S. (not significant): denote a result from a statistical hypothesis-testing procedure that does not allow the researcher to conclude that differences in the data obtained for different samples are meaningful.

	PC = 92	**PL = 26**	**BPH = 49**	**SIGNIFICANCE**
AGE	70 ± 7.86	68 ± 7.87	65 ± 8.17	** $p = 0.009$
PSA	21.28 ± 45.09	6.38 ± 4.57	6.87 ± 6.80	** $p = 0.0013$
INDEX	12 ± 5.59	20 ± 11.11	19.48 ± 10.18	* $p = 0.009$, ** $p = 0.007$
WBC	7.73 ± 2.14	6.46 ± 1.45	7.33 ± 2.26	N.S.
RBC	5.07 ± 0.59	5.18 ± 0.93	5.24 ± 0.51	N.S.
HGB	14.20 ± 1.64	14.67 ± 2.16	14.75 ± 1.26	N.S.
RDW	13.99 ± 1.51	13.51 ± 0.95	13.60 ± 0.99	N.S.
HDW	2.64 ± 0.41	2.55 ± 0.35	2.52 ± 0.30	N.S.
PLT	235.5 ± 66.15	217.35 ± 45.01	235.60 ± 55.80	N.S.
NEUT	4.88 ± 1.89	3.96 ± 1.33	4.45 ± 1.91	N.S.
LYMPH	1.97 ± 0.79	1.77 ± 0.50	2.04 ±0.79	N.S.
MONO	0.50 ± 0.17	0.43 ± 0.13	0.47 ± 0.15	N.S.
EOS	0.20 ± 0.14	0.17 ± 0.10	0.23 ± 0.15	N.S.
BASO	0.04 ± 0.05	0.02 ± 0.04	0.04 ± 0.05	N.S.
LUC#	0.14 ± 0.07	0.12 ± 0.04	0.14 ± 0.06	N.S.
LUC%	1.96 ± 0.73	2.03 ± 0.57	2.13 ± 0.74	N.S.
LMR	4.16 ± 1.50	4.49 ± 1.80	4.47 ± 1.40	N.S.
NLR	2.92 ± 1.85	2.51 ± 1.67	2.47 ± 1.24	N.S.
PLR	137.69 ± 63.58	131.05 ± 42.02	132.45 ± 58.93	N.S.
SIRI	1.50 ± 1.28	1.15 ± 0.99	1.19 ± 0.94	N.S.
AISI	367.07 ± 338.04	247.24 ± 206.44	292.39 ± 289.63	N.S.
PSA/AISI%	0.10 ± 0.26	0.04 ± 0.03	0.04 ± 0.04	N.S.
INDEX/SIRI	11.75 ± 11.98	24.10 ± 29.58	12.49 ± 15.34	N.S.
INDEX/AISI%	0.06 ± 0.07	0.12 ± 0.16	0.06 ± 0.07	N.S.

Table 1. *Cont.*

	PC = 92	PL = 26	BPH = 49	SIGNIFICANCE
FAMILIARITY	8/92 (8.69%)	6/26 (23.07%)	6/49 (12.24%)	N.S.
CHARLSON	5.22 ± 1.62	2.47 ± 1.19	2.75 ± 1.37	* $p = 0.02$, ** $p = 0.013$
G6PDH DEFICIT	7/92 (7.60%)	3/26 (11.53%)	5/49 (10.2%)	N.S.
BMI	27.40 ± 3.67	26.87 ± 2.82	26.80 ± 4.01	N.S.
IPSS	11.88 ± 6.43	12 ± 8.51	12.93 ± 9.47	N.S.
IIEF	13.06 ± 7.40	17.29 ± 6.17	15.75 ± 8.43	* $p = 0.02$
TRUS	51.26 ± 24.98	60.31 ± 33.05	65.45 ± 35.46	** $p = 0.009$
SMOKE	32/92 (34.78%)	4/26 (15.38%)	13/49 (26.53%)	N.S.
ALCOHOL	1/92 (1.09%)	0/26 (0%)	2/49 (4.08%)	N.S.

2.3. Arginine Decarboxylase (ADC) Quantification

The concentration of human arginine decarboxylase was evaluated using Human ADC (Arginine decarboxylase) ELISA Kit (Nordic Bioscience AB, Propellervägen, Sweden). Plate was washed twice before starting experiments according to the manufacturer's instructions. After washing, 100 µL of each sample was incubated in a pre-treated plate at 37 °C for 90 min. After two washing steps in washing buffer, 100 µL Biotin-labelled antibody working solution was added in each well and incubated incubate at 37 °C for 60 min. Antibody was then removed and replaced by HRP-Streptavidin Conjugate solution for 30 min at 37 °C. After several washing steps, TMB liquid substrate was incubated at 37 °C in dark for 20 min and then stopped by the stop solution provided by the kit. Colour development was analysed at 450 nm using a microplate reader (Akribis Scientific, Common Farm, Frog Ln, Knutsford WA16 0JG, Great Britain). Standard curves were prepared according to manufacturer's instructions. The relative O.D.450 of each sample was expressed as the (O.D.450 of each well) − (the O.D.450 of blank well). Each sample was assayed in duplicate, and values were expressed as the mean ± SD of 2 measures per sample.

2.4. Statistical Analysis

Results are expressed as an average value (mean ± DS). The distribution of variables was evaluated using the Kruskal–Wallis test and applied in order to compare the groups. The Kruskal–Wallis rank sum was employed to evaluate the distributions of each variance in the three groups under observation, assuming the value $p < 0.05$ as statistically significant. Statistical comparisons among the groups of parametric variables were evaluated using the unpaired Student t-test. The non-parametric continuous variables were compared with the case of normally distributed samples and with the median ± median absolute deviation (MAD) in the case of non-normal sample distribution. Correlations among variables were estimated using Pearson correlation. To verify the presence of associations among variables potentially involved in the development of the disease, a logistic regression analysis was performed. The analysis of the receiver operational characteristics curve (ROC) was used to test the ability of polyamines to predict prostate cancer. ROC curves were obtained by calculating the area under the curve (AUC). A supervised analysis was carried out by applying the orthogonal partial discriminant analysis of the minimum square (OPLS-DA), representing a rotation of the corresponding PLS-DA models and simplifying the information in a only one predictive component while maintaining the same predictive capacity [53]. To avoid model overfitting, the corresponding PLS-DA models were validated by 300-fold permutation tests. The prediction strength of the model was evaluated by "Leave out" analysis. Variable Importance Parameter (VIP) values were used to assess the overall contribution of each X variable to the model, summed over all components and weighted according to the Y variation accounted for by each component. The number of terms in the sum depends on the number of PLS-DA components found to be

significant in distinguishing the classes. The Y-axis indicates the VIP scores corresponding to each variable on the X-axis. Bars indicate the factors with the highest VIP scores, and thus are the most contributory variables in class discrimination in the PLS-DA model. Comparison of univariate peaks was performed for the integrals of distinct metabolites using the non-parametric Mann–Whitney U analysis. The statistical analysis was carried out using Statgraphics Centurion XVII (v.17.2) software, MedCalc for Windows, version 15.4 64 bit (MedCalc Software, Ostend, Belgium), and SIMCA-P version 13.0, (Umetrics AB, Umea, Sweden) [54].

3. Results

3.1. Clinical Data

Table 1 shows the most important clinical information of the patients, including age, body mass index, lifestyle habits (smoking, alcohol), family history of prostate cancer, total serum PSA, serum PSA index, blood cell counts (WBC, RBC, HGB, PLT), leukocyte counts (Lymphocytes, Neutrophils, Monocytes), plasma inflammatory indices (MRL, NLR, PLR), and combined plasma inflammatory indices (SIRI, AISI), Charlson comorbidities, G6PD, IPSS (international prostatic symptoms score), IIEF (international index of erectile function), and TRUS (trans rectal ultrasound).

Average age of PC patients was 70 $\pm$ 7.86 years, PL patients 68 $\pm$ 7.87 and BPH patients 65 $\pm$ 8.17, showing that patients were aged from 57 to 77.

In the total sample, the most common pathological change in the prostate was prostate cancer in 55.10% of cases, followed by BPH in 29.34% of cases, precancerous conditions (atypical small acinar proliferation—ASAP—and high-grade prostatic intraepithelial neoplasia—HGPIN) in 15.57% of cases, and atrophic and inflammatory changes in the prostate in 14.1 % of cases. Based on the diagnosis, patients were divided into three groups. The age distribution of pathological changes in the prostate demonstrates that patients with prostate cancer were the oldest, with an average age of 70 years, followed by patients with precancerous conditions (HGPIN and ASAP) with 68 years, while the youngest were patients with BPH, with an average age of 65 years. Total PSA values were significantly different between PC patients and BPH. The analysis by Kruskal–Wallis test indicates that there is a significant difference, with increasing age, in Charlson and a decrease in TRUSS between prostate cancer and benign prostatic hyperplasia.

The correlation between PC patients and PL patients for PSA exhibits an increasing trend, while those for Charlson and IIEF exhibit a decreasing trend.

3.2. Polyamine Analysis

Table 2 shows the levels of plasma polyamines, and of the related amino acids (arginine, lysine) and metabolites (GABA) in the three groups. Patients with prostate cancer exhibited a significant increase in GABA, spermine, spermidine, putrescine, cadaverine and lysine levels as compared to Pl patients. An opposite trend could be observed for agmatine and acetyl-putrescine levels.

Values of agmatine and acetyl putrescine were significantly decreased, while GABA, spermine, spermidine, putrescine, cadaverine, lysine and ornithine levels were increased, in PC patients as compared to BPH. The analysis by Kruskal–Wallis test indicated that there was a significant difference in the observed changes (Figure 1).

3.3. Mono and Multivariate Analysis

In Figure 1, the multivariate analysis using the PLS-DA method (partial least squares discriminant analysis) shows good discrimination between the three groups of samples; in Figure 2, the OPLS-DA—orthogonal partial least squares discriminant analysis—reports the score plots derived from the LC-HRMS spectra of the plasma and the corresponding loading plots of the coefficients obtained from the three groups. The orthogonal matrix makes it possible to explore the 'orthogonal' components more easily and to fully understand data set. The characteristics of the OPLS method have been investigated for the purpose

of discriminant analysis (OPLS-DA), demonstrating that class-orthogonal variation can be exploited to increase classification performance in those cases in which the individual classes exhibit divergence with respect to within-class variation [52].

Table 2. Level of plasma polyamines, plasma correlated amino acids (arginine, lysine) and metabolites (GABA) (ng/mL). * PC vs. PL, ** PC vs. BPH, *** BPH vs. PL.

POLYAMINES	PC	PL	BPH	SIGNIFICANCE
AGMATINE	39.9 ± 12.06	55.31 ± 15.27	77.62 ± 15.05	* $p = 0.007$, ** $p = 0.01$, *** $p = 0.009$
GABA	30.03 ± 14.97	16.83 ± 12.54	22.02 ± 13.41	* $p = 0.01$, ** $p = 0.008$
SPERMINE	3.74 ± 2.20	2.8 ± 1.94	2.97 ± 1.76	* $p = 0.01$, ** $p = 0.01$
SPERMIDINE	8.43 ± 3.03	7.02 ± 1.78	5.31 ± 1.49	* $p = 0.009$, ** $p = 0.007$, *** $p = 0.01$
PUTRESCINE	14.28 ± 8.43	7.56 ± 1.62	6.45 ± 2.21	* $p = 0.01$, ** $p = 0.01$, *** $p = 0.01$
ACETYLPUTRESCINE	0.06 ± 0.04	0.14 ± 0.17	0.16 ± 0.10	* $p = 0.008$, ** $p = 0.01$
ACETYLSPERMINE	2.42 ± 0.77	2.68 ± 1.33	2.27 ± 0.49	*** $p = 0.007$
ACETYLSPERMIDINE	0.35 ± 0.24	0.4 ± 0.27	0.38 ± 0.24	N.S.
CADAVERINE	2.53 ± 0.81	1.75 ± 0.68	1.75 ± 0.67	* $p = 0.01$, ** $p = 0.01$
ARGININE	$6.02 \pm 2.30 \times 10^4$	5.59 ± 1.87	5.39 ± 1.88	N.S.
LYSINE	$2.33 \pm 0.86 \times 10^4$	1.64 ± 0.58	6.93 ± 2.06	* $p = 0.006$, ** $p = 0.01$
ORNITHINE	$0.83 \pm 0.29 \times 10^4$	0.91 ± 0.17	1.04 ± 0.41	** $p = 0.01$

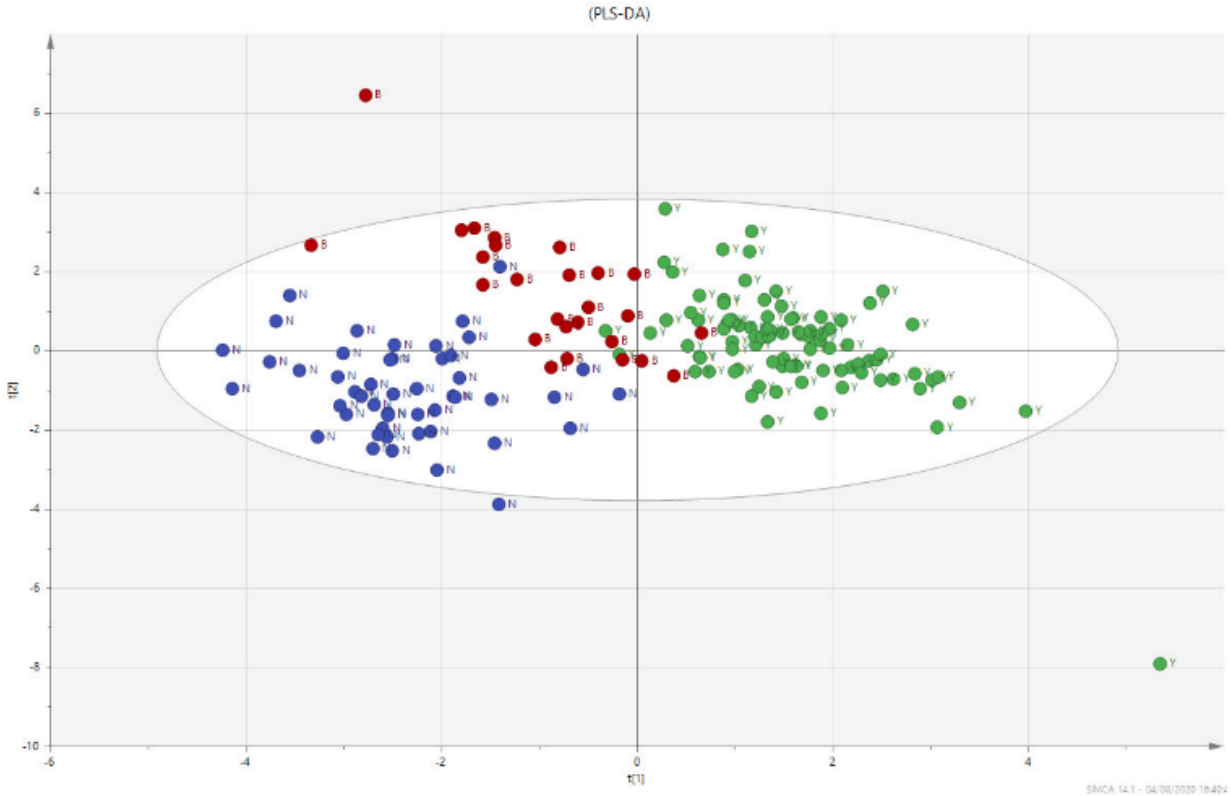

Figure 1. Multivariate analysis using PLS-DA method. PLS-DA loading plot shows a good dis-crimination of the three groups of samples, PC (GREEN), the PL group (RED) and the BPH group (BLUE).

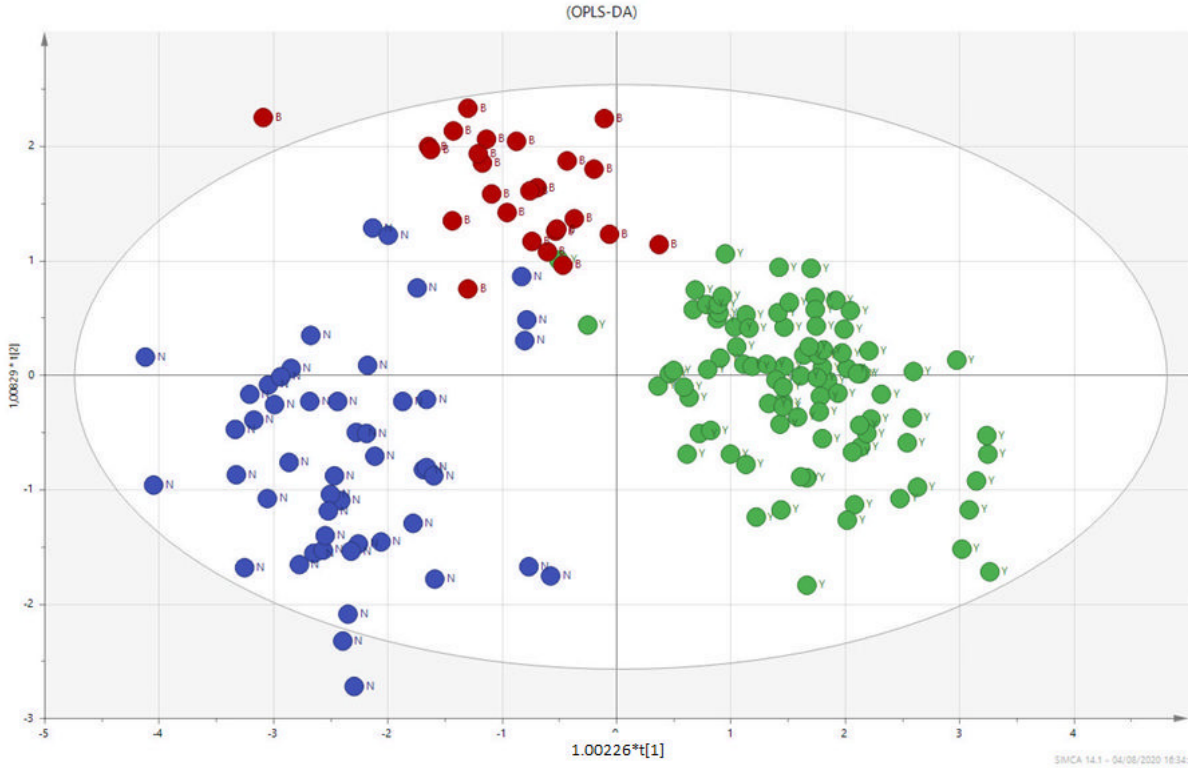

Figure 2. PLS-DA score plots derived from the LC-HRMS spectra of plasma and corresponding coefficient loading plots obtained from the three groups—PC (GREEN), PL (RED), and BPH (BLUE).

The supervised analysis was performed by applying orthogonal partial least squares discriminant analysis (OPLS-DA), which implies a rotation of the corresponding PLS-DA models and simplifies the concentration of information into one predictive component while maintaining the same predictive ability [53]. We found that patients in the different groups were distributed in different areas, which indicated the significant difference in the metabolic mode between the group with PC (GREEN), the PL group (RED), and the BPH group (BLUE). Figures 1 and 2 show the corresponding 2D predictive scoring plot against the first orthogonal component; the three groups tended to cluster naturally. Compared to the unsupervised principal component analysis, the supervised OPLS-DA makes it possible to obtain the variables' influence on projection (VIP), highlighting the differences between the groups (Figures 3 and 4).

VIP is a parameter used to calculate the cumulative measure of the influence of individual X-variables on the model. Variable influence on projection is applied in multivariate clinical data analysis to achieve improved diagnosis of process dynamics. Variable influence on projection (VIP) is commonly used to summarise the importance of the X-variables in multivariate models based on projections to latent structures, e.g., the PLS and OPLS methods. VIP values as great as or greater than 1 point to the most relevant variables, and generally, VIP values below 0.5 are considered to be irrelevant variables. Thus, VIP for OPLS with positive contribution scores corresponds to the metabolites contributing to class discrimination in the OPLS-DA model. The number of terms in the sum depends on the number of OPLS-DA components that are significant for distinguishing classes. The Y-axis shows the VIP scores corresponding to each variable on the X-axis. To avoid model overfitting, the corresponding OPLS-DA models were validated by 300-fold permutation tests, shown in Figure 5. The resulting regression lines showed an intercept of R2 at 0.0249 and an intercept of Q2 at −0.246, indicating the validity of the model. This difference was maintained when the paired analysis of the samples from three groups was split. Based on the OPLS-DA results, there was a statistically significant difference between the three classes of patients. The scoring plot of the predictive component showed no overlap.

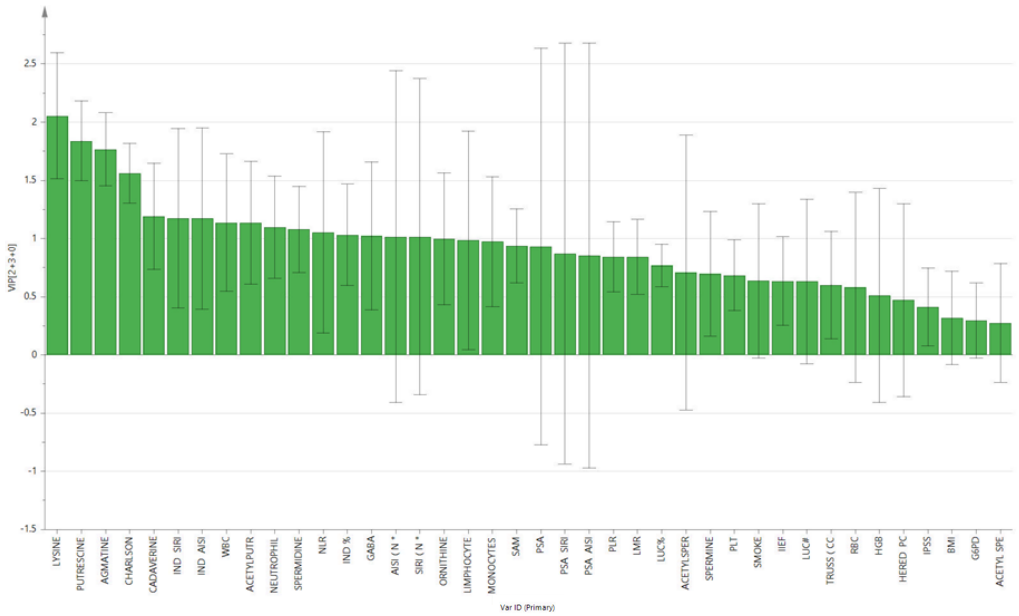

Figure 3. Contribution plot from model including total VIP; peaks with positive contribution scores correspond to metabolites with higher levels. The Y-axis indicates the VIP scores corresponding to each variable on the X-axis.

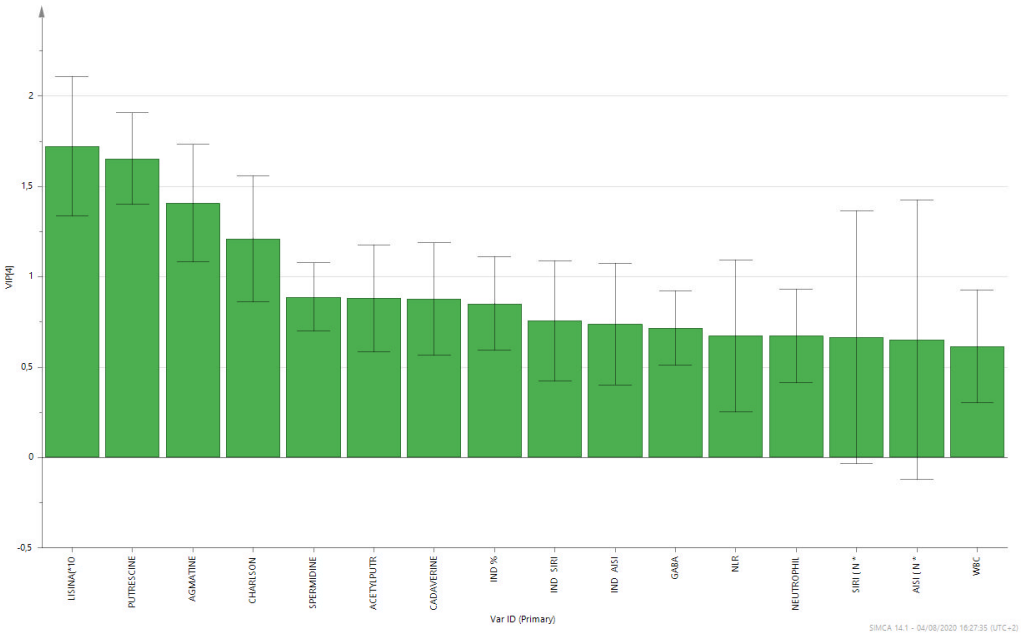

Figure 4. Factors with the highest VIP scores and contributory variables in class discrimination in the PLS-DA model.

The accuracy for the optimal cut-off of biomarkers predicting disease progression (combined with pathological variables) was determined using ROC curves (Figure 6) and by univariate analysis (Supplementary Materials). ROC curves were used to quantify the predictive accuracy of the metabolites. We observed no significant differences between the three groups using the ROC curves calculated for ornithine, acetyl-spermidine, spermine and acetyl-spermine; increased levels of cadaverine were observed in PC patients, while there was no significant difference between BPH patients and PL. ROC curves of putrescine and spermidine are indeed able to discriminate between PC and PL, while acetyl-putrescine significantly decreases in PC groups (Supplementary Materials). The predictive ability

of PSA was analysed using the ROC curves. The area under the ROC curve and its 95% confidence intervals for PSA are shown in Figure S10 in the Supplementary Materials. The area under the curve for PSA is 0.685. Comparison of PSA among the three groups revealed no statistically significant differences. Analysis of the agmatine panel shows an AUC of 0.959 and $p \leq 0.001$ when differentiating between PC and BPH patients (Figure 6).

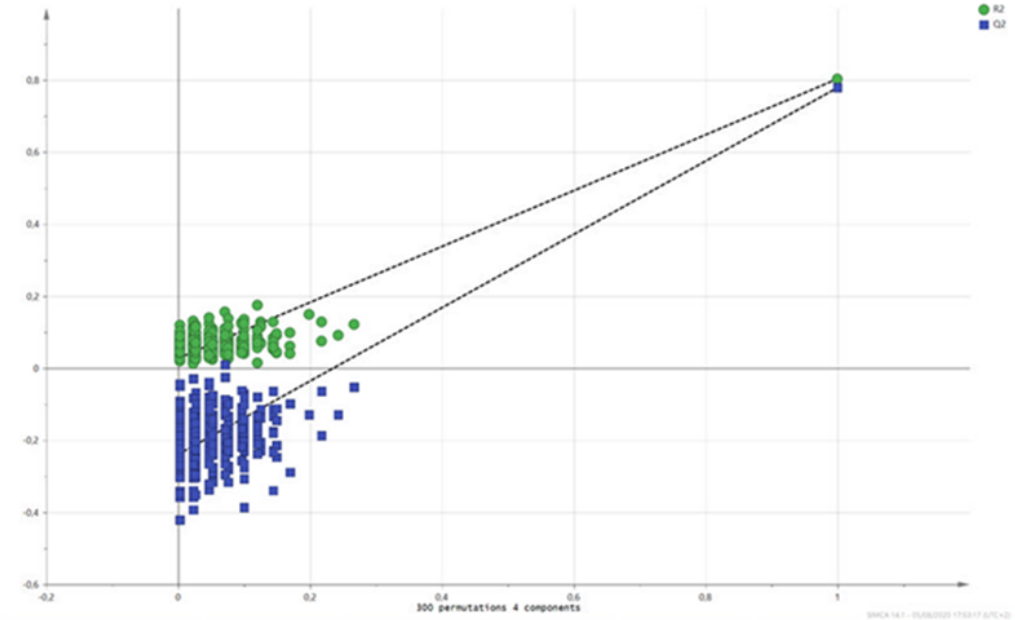

	Members	Correct	Y	N	B	No class (YPred <= 0)
PC	91	98.90%	90	0	1	0
BPH	50	94.00%	0	47	3	0
PL	26	92%	1	1	24	0
No class	2		0	1	1	0
Total	169	96.41%	91	49	29	0
Fisher's prob.	6.10E-07					

Figure 5. Validation method: 300-fold cross permutation validation plot. The Y-axis represents R2 (triangles) and Q2 (circles) for the model, and the X-axis designates the correlation coefficient between original and permuted response data.

3.4. Arginine Decarboxylase (ADC) Quantification

The concentration of ADC, an enzyme responsible for catalysing the conversion of L-arginine to agmatine and carbon dioxide, was quantified in the plasma of the PC, PL and BPH patient groups. Figure 7 shows an increase in ADC concentration in PL and BPH patients compared to PC patients, confirming the trend in plasma agmatine levels.

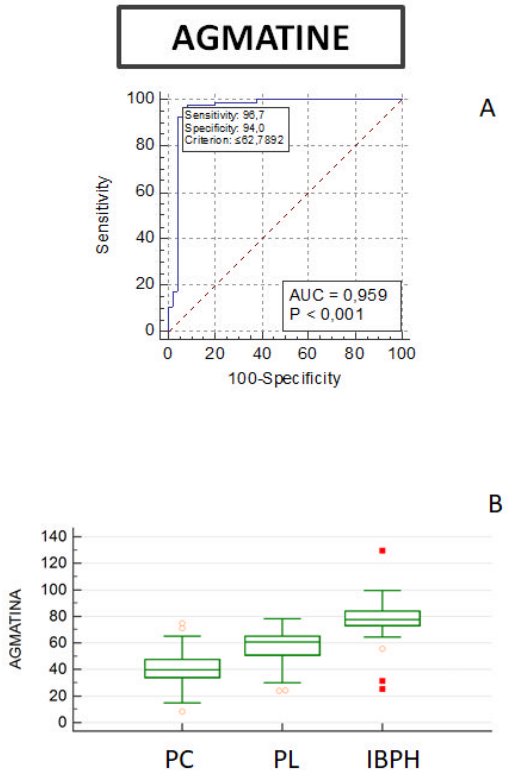

Figure 6. (**A**) ROC curve diagram of agmatine sensitivity and specificity in prediction of pathological conditions in PC and BPH patients. (**B**) Boxplots showing the distribution of agmatine among subjects with prostate cancer (PC, n = 92), precancerous lesions (PL, n = 26), or benign prostatic hyperplasia (BPH, n = 49). The centre line of the boxplots indicates the median (limits of the box indicate the 25th and 75th percentile). The whiskers represent either 1.5 times the interquartile range (IQR) or the maximum/minimum data point if they are within 1.5 times the IQR. Wilcoxon's test was used to compare mean agmatine levels among groups.

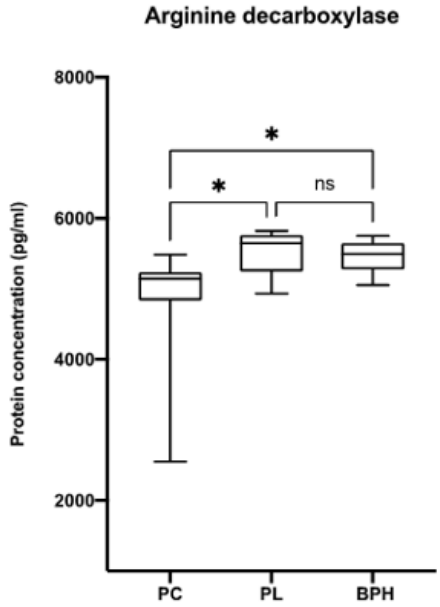

Figure 7. Arginine decarboxylase (ADC) quantification by ELISA. The concentration of ADC was measured in the plasma of patients from each group. Data are expressed as mean ± SD with reference to the control (mean ± SD; n = 170) (* $p \leq 0.05$).

4. Discussion

Among the metabolites tested, agmatine, in terms of sensitivity and specificity, was significantly different among the three groups. This increase was further confirmed by the observed increase in arginine decarboxylase activity levels in PL and BPH compared to PC (Figure 7) [55,56]. Different authors have demonstrated that agmatine is able to inhibit polyamine synthesis by increasing the expression of antizyme mediating the degradation of ornithine de-carboxylase and increasing the spermidine–spermine acetyl transferase activity [55,57–60]. On the other hand, decreased polyamine levels, observed by us in PL and BPH patients, could stabilise the transcripts (p53, TGF-β, JunD) of the genes inhibiting growth [59–64]. The observed agmatine level trend in plasma fit perfectly with previous results described by other authors in different kinds of tumour [65].

Agmatine is derived from arginine by the action of arginine decarboxylase. Many studies have shown that arginine is an important player in a variety of different biological processes, such as cell growth, and becomes a limiting factor in states of rapid turnover (e.g., neoplasms). Arginine deprivation therapy is being investigated as an adjuvant therapy for cancer; however, arginine is also required for the immune destruction of malignant cells [66,67]. Agmatine, with is a derivative of arginine that is irregularly distributed in organs and tissues, has a dual behaviour. On one hand, it interferes with polyamine synthesis by reducing the activity of ornithine decarboxylase (ODC), while on the other hand, it inhibits the uptake of polyamines [68,69]; this interference in turn leads to the suppression of tumour cell proliferation in vitro [57,70]. In this context, other authors have also shown that agmatine inhibits the proliferation of cancer cell lines in vivo by interfering with the polyamine pathway [71]. Our results support evidence of a promising plasma biomarker for prostate cancer patients that could be used in current medical practice to reduce unnecessary biopsies. Analysis of ROC curves showed that variations in agmatine concentrations, in terms of sensitivity and specificity, may be promising discriminators among the three groups of patients examined.

5. Conclusions

The data collected in this study and their statistical analysis suggest effective correlations between variations in indices of systemic inflammation and polyamine levels, al-lowing classification of the three categories of patients examined. The data obtained encourage us to further explore the use of promising biomarkers of disease progression in future clinical practice to differentiate patients into diagnostic classes and identify high-risk patients at an early stage. The results not only contribute to the understanding of prostate cancer, but also increase the knowledge of the complex interrelationships between polyamine metabolism and tumour cell proliferation, also in relation to the possible role played by the microenvironment surrounding the tumour.

Supplementary Materials: The following supporting information can be downloaded at: https://www.mdpi.com/article/10.3390/biom12040514/s1, ROC curve PC vs. PL + BPH. Receiver operating characteristic (ROC) curve. The closer the curve is to the upper left corner of each graph, the better is the classifier compared to chance. Figure S1: Acetylputrescine. ROC curve diagram of Acetylputrescine sensitivity and specificity in prediction of pathological conditions in patients PC and BPH. Boxplots showing the distribution of Acetylputrescine among subjects with prostate cancer (PC, N = 92), precancerous lesions (PL, N = 26), or benign prostatic hyperplasia (BPH, N = 49). The centre line of the boxplots indicates the median (limits of the box indicate the 25th and 75th percentile). The whiskers represent either 1.5 times the interquartile range (IQR) or the maximum/minimum data point if they are within 1.5 times the IQR. Wilcoxon's test was used to compare mean Agmatine levels among groups. Figure S2: Acetylspermidine. ROC curve diagram of Acetylspermidine sensitivity and specificity in prediction of pathological conditions in patients PC and BPH. Boxplots showing the distribution of Acetylspermidine among subjects with prostate cancer (PC, N = 92), precancerous lesions (PL, N = 26), or benign prostatic hyperplasia (BPH, N = 49). The centre line of the boxplots indicates the median (limits of the box indicate the 25th and 75th percentile). The whiskers represent either 1.5 times the interquartile range (IQR) or the maximum/minimum data point if they are

within 1.5 times the IQR. Wilcoxon's test was used to compare mean Agmatine levels among groups. Figure S3: Acetylspermine. ROC curve diagram of Acetylspermidine sensitivity and specificity in prediction of pathological conditions in patients PC and BPH. Boxplots showing the distribution of Acetylspermine among subjects with prostate cancer (PC, N = 92), precancerous lesions (PL, N = 26), or benign prostatic hyperplasia (BPH, N = 49). The centre line of the boxplots indicates the median (limits of the box indicate the 25th and 75th percentile). The whiskers represent either 1.5 times the interquartile range (IQR) or the maximum/minimum data point if they are within 1.5 times the IQR. Wilcoxon's test was used to compare mean Agmatine levels among groups. Figure S4: Cadaverine. ROC curve diagram of Cadaverine sensitivity and specificity in prediction of pathological conditions in patients PC and BPH. Boxplots showing the distribution of Cadaverine among subjects with prostate cancer (PC, N = 92), precancerous lesions (PL, N = 26), or benign prostatic hyperplasia (BPH, N = 49). The centre line of the boxplots indicates the median (limits of the box indicate the 25th and 75th percentile). The whiskers represent either 1.5 times the interquartile range (IQR) or the maximum/minimum data point if they are within 1.5 times the IQR. Wilcoxon's test was used to compare mean Agmatine levels among groups. Figure S5: Lysine. ROC curve diagram of Lysine sensitivity and specificity in prediction of pathological conditions in patients PC and BPH. Boxplots showing the distribution of Lysine among subjects with prostate cancer (PC, N = 92), precancerous lesions (PL, N = 26), or benign prostatic hyperplasia (BPH, N = 49). The center line of the boxplots indicates the median (limits of the box indicate the 25th and 75th percentile). The whiskers represent either 1.5 times the interquartile range (IQR) or the maximum/minimum data point if they are within 1.5 times the IQR. Wilcoxon's test was used to compare mean Agmatine levels among groups. Figure S6: Ornithine. ROC curve diagram of Ornithine sensitivity and specificity in prediction of pathological conditions in patients PC and BPH. Boxplots showing the distribution of Ornithine among subjects with prostate cancer (PC, N = 92), precancerous lesions (PL, N = 26), or benign prostatic hyperplasia (BPH, N = 49). The center line of the boxplots indicates the median (limits of the box indicate the 25th and 75th percentile). The whiskers represent either 1.5 times the interquartile range (IQR) or the maximum/minimum data point if they are within 1.5 times the IQR. Wilcoxon's test was used to compare mean Agmatine levels among groups. Figure S7: Putrescine. ROC curve diagram of Putrescine sensitivity and specificity in prediction of pathological conditions in patients PC and BPH. Boxplots showing the distribution of Putrescine among subjects with prostate cancer (PC, N = 92), precancerous lesions (PL, N = 26), or benign prostatic hyperplasia (BPH, N = 49). The center line of the boxplots indicates the median (limits of the box indicate the 25th and 75th percentile). The whiskers represent either 1.5 times the interquartile range (IQR) or the maximum/minimum data point if they are within 1.5 times the IQR. Wilcoxon's test was used to compare mean Agmatine levels among groups. Figure S8: Spermidine. ROC curve diagram of Spermidine sensitivity and specificity in prediction of pathological conditions in patients PC and BPH. Boxplots showing the distribution of Spermidine among subjects with prostate cancer (PC, N = 92), precancerous lesions (PL, N = 26), or benign prostatic hyperplasia (BPH, N = 49). The center line of the boxplots indicates the median (limits of the box indicate the 25th and 75th percentile). The whiskers represent either 1.5 times the interquartile range (IQR) or the maximum/minimum data point if they are within 1.5 times the IQR. Wilcoxon's test was used to compare mean Agmatine levels among groups. Figure S9: Spermine. ROC curve diagram of Spermine sensitivity and specificity in prediction of pathological conditions in patients PC and BPH. Boxplots showing the distribution of Spermine among subjects with prostate cancer (PC, N = 92), precancerous lesions (PL, N = 26), or benign prostatic hyperplasia (BPH, N = 49). The center line of the boxplots indicates the median (limits of the box indicate the 25th and 75th percentile). The whiskers represent either 1.5 times the interquartile range (IQR) or the maximum/minimum data point if they are within 1.5 times the IQR. Wilcoxon's test was used to compare mean Agmatine levels among groups. Figure S10: PSA. ROC curve diagram of PSA sensitivity and specificity in prediction of pathological conditions in patients PC and BPH. Boxplots showing the distribution of PSA among subjects with prostate cancer (PC, N = 92), precancerous lesions (PL, N = 26), or benign prostatic hyperplasia (BPH, N = 49). The center line of the boxplots indicates the median (limits of the box indicate the 25th and 75th percentile). The whiskers represent either 1.5 times the interquartile range (IQR) or the maximum/minimum data point if they are within 1.5 times the IQR. Wilcoxon's test was used to compare mean Agmatine levels among groups.

Author Contributions: Conceptualisation, D.C. and C.C.; methodology, D.C. and E.A.; software, D.C. and E.A.; validation, D.C., E.A., N.C., A.Z.; formal analysis, D.C.; investigation, D.C., S.C. and E.A., T.S.; resources, M.M. (Massimo Madonia) and T.S.; data curation, D.C., A.Z. and N.C.; writing—original draft preparation, D.C.; writing—review and editing, S.M. and M.M. (Margherita Maioli); supervision, C.C., M.M. (Margherita Maioli); funding acquisition, M.M. (Massimo Madonia); All authors have read and agreed to the published version of the manuscript.

Funding: Funding support was provided by FAR UNISS 2020, and by Fondazione di Sardegna U660.2022/AI.645.BE prat. 2022.0788.

Institutional Review Board Statement: The study was conducted in accordance with the Declaration of Helsinki.

Informed Consent Statement: Informed consent was obtained from all subjects involved in the study.

Conflicts of Interest: The authors declare no conflict of interest. The authors declare that they have no known competing financial interests or personal relationships that could have appeared to influence the work reported in this paper.

Abbreviations

ADC	arginine decarboxylase
AISI	(neutrophils × monocytes × platelets)/lymphocyte ratio
AO-Agm	isosteric-agmatine hydroxylamine analogue
APAO	acetylated polyamine oxidase
ASAP	Atypical Small Acinar Proliferation
AUC	area under the curve
BPH	benign prostatic hyperplasia
Cad	cadaverine
CTC	circulating cancer cells
1,3-DAP	1,3-diaminopropane
dcAdoMet	decarboxylated S-adenosyl-l-methionine
DRE	digital rectal examination
HBFA	heptafluorobutyric acid
IIEF	international index of erectile function
IPSS	international prostatic symptoms score
LC-HRMS	Liquid Chromatography-High Resolution Mass Spectrometry
LDC	lysine decarboxylase
MAD	median ± median absolute deviation
MLR	monocyte/lymphocyte ratio
NLR	neutrophil/lymphocyte ratio
dNLR	derived NLR [dNLR = neutrophils/(white blood cells − neutrophils)]
NO	nitric oxide
ODC	ornithine decarboxylase
OPLS-DA	orthogonal partial discriminant analysis of the minimum squares
Orn	ornithine
PAs	polyamines
PAOs	polyamine oxidases
PC	prostate cancer
PHI	prostate health index
PIN	prostatic intraepithelial neoplasia
PL	precancerous lesion
PLR	platelet/lymphocyte ratio
PLS-DA	partial least squares discriminant analysis
PSA	prostate-specific antigen

fPSA	free PSA
proPSA	PSA precursors
tPSA	total PSA
Put	putrescine
QC	quality control
ROC	receiver operational characteristics curve
SIRI	(neutrophils × monocytes)/lymphocyte ratio
Spd	spermidine
SpdS	spermidine synthase
Spm	spermine
SpmS	spermine synthase
SSAT	spermidine/spermine acetyltransferase
TRUS	trans rectal ultrasound
VIP	variable importance parameter

References

1. Rawla, P. Epidemiology of prostate cancer. *World J. Oncol.* **2019**, *10*, 63. [CrossRef] [PubMed]
2. Hamilton, W.; Sharp, D. Symptomatic diagnosis of prostate cancer in primary care: A structured review. *Br. J. Gen. Pr.* **2004**, *54*, 617–621.
3. Boyle, H.; Alibhai, S.; Decoster, L.; Efstathiou, E.; Fizazi, K.; Mottet, N.; Oudard, S.; Payne, H.; Prentice, M.; Puts, M.; et al. Updated recommendations of the International Society of Geriatric Oncology on prostate cancer management in older patients. *Eur. J. Cancer* **2019**, *116*, 116–136. [CrossRef]
4. Hoffman, R.M. Screening for prostate cancer. *N. Engl. J. Med.* **2011**, *365*, 2013–2019. [CrossRef]
5. Catalona, W.J.; Smith, D.S.; Ratliff, T.L.; Dodds, K.M.; Coplen, D.E.; Yuan, J.J.J.; Petros, J.A.; Andriole, G.L. Measurement of Prostate-Specific Antigen in Serum as a Screening Test for Prostate Cancer. *N. Engl. J. Med.* **1991**, *324*, 1156–1161. [CrossRef] [PubMed]
6. Catalona, W.J.; Partin, A.W.; Sanda, M.G.; Wei, J.T.; Klee, G.G.; Bangma, C.H.; Slawin, K.M.; Marks, L.S.; Loeb, S.; Broyles, D.L. A multicenter study of [-2] pro-prostate specific antigen combined with prostate specific antigen and free prostate specific antigen for prostate cancer detection in the 2.0 to 10.0 ng/mL prostate specific antigen range. *J. Urol.* **2011**, *185*, 1650–1655. [CrossRef] [PubMed]
7. Kale, M.S.; Korenstein, D. Overdiagnosis in primary care: Framing the problem and finding solutions. *BMJ* **2018**, *362*, k2820. [CrossRef]
8. Campos-Fernández, E.; Barcelos, L.S.; De Souza, A.G.; Goulart, L.R.; Alonso-Goulart, V. Research landscape of liquid biopsies in prostate cancer. *Am. J. Cancer Res.* **2019**, *9*, 1309–1328.
9. Cooperberg, M.R.; Simko, J.P.; Cowan, J.E.; Reid, J.E.; Djalilvand, A.; Bhatnagar, S.; Gutin, A.; Lanchbury, J.S.; Swanson, G.P.; Stone, S.; et al. Validation of a Cell-Cycle Progression Gene Panel to Improve Risk Stratification in a Contemporary Prostatectomy Cohort. *J. Clin. Oncol.* **2013**, *31*, 1428–1434. [CrossRef]
10. De Bono, J.S.; Scher, H.I.; Montgomery, R.B.; Parker, C.; Miller, M.C.; Tissing, H.; Doyle, G.V.; Terstappen, L.W.W.M.; Pienta, K.J.; Raghavan, D. Circulating Tumor Cells Predict Survival Benefit from Treatment in Metastatic Castration-Resistant Prostate Cancer. *Clin. Cancer Res.* **2008**, *14*, 6302–6309. [CrossRef]
11. Cohen, J.D.; Javed, A.A.; Thoburn, C.; Wong, F.; Tie, J.; Gibbs, P.; Schmidt, C.M.; Yip-Schneider, M.T.; Allen, P.J.; Schattner, M.; et al. Combined circulating tumor DNA and protein biomarker-based liquid biopsy for the earlier detection of pancreatic cancers. *Proc. Natl. Acad. Sci. USA* **2017**, *114*, 10202–10207. [CrossRef] [PubMed]
12. Cohen, J.D.; Li, L.; Wang, Y.; Thoburn, C.; Afsari, B.; Danilova, L.; Douville, C.; Javed, A.A.; Wong, F.; Mattox, A.; et al. Detection and localization of surgically resectable cancers with a multi-analyte blood test. *Science* **2018**, *359*, 926–930. [CrossRef] [PubMed]
13. Greten, F.R.; Grivennikov, S.I. Inflammation and cancer: Triggers, mechanisms, and consequences. *Immunity* **2019**, *51*, 7–41. [CrossRef] [PubMed]
14. Murata, M. Inflammation and cancer. *Environ. Health Prev. Med.* **2018**, *23*, 1–8. [CrossRef] [PubMed]
15. Klein, E.A.; Cooperberg, M.R.; Magi-Galluzzi, C.; Simko, J.P.; Falzarano, S.M.; Maddala, T.; Chan, J.M.; Li, J.; Cowan, J.E.; Tsiatis, A.C. A 17-gene assay to predict prostate cancer aggressiveness in the context of gleason grade heterogeneity, tumor multifocality, and biopsy undersampling. *Eur. Urol.* **2014**, *66*, 550–560. [CrossRef] [PubMed]
16. Knezevic, D.; Goddard, A.D.; Natraj, N.; Cherbavaz, D.B.; Clark-Langone, K.M.; Snable, J.; Watson, D.; Falzarano, S.M.; Magi-Galluzzi, C.; Klein, E.A. Analytical validation of the oncotype dx prostate cancer assay—A clinical rt-pcr assay optimized for prostate needle biopsies. *BMC Genom.* **2013**, *14*, 1–12. [CrossRef]
17. Cullen, J.; Rosner, I.L.; Brand, T.C.; Zhang, N.; Tsiatis, A.C.; Moncur, J.; Ali, A.; Chen, Y.; Knezevic, D.; Maddala, T.; et al. A Biopsy-based 17-gene Genomic Prostate Score Predicts Recurrence After Radical Prostatectomy and Adverse Surgical Pathology in a Racially Diverse Population of Men with Clinically Low- and Intermediate-risk Prostate Cancer. *Eur. Urol.* **2015**, *68*, 123–131. [CrossRef]

18. Parekh, D.J.; Punnen, S.; Sjoberg, D.D.; Asroff, S.W.; Bailen, J.L.; Cochran, J.S.; Concepcion, R.; David, R.D.; Deck, K.B.; Dumbadze, I.; et al. A Multi-institutional Prospective Trial in the USA Confirms that the 4Kscore Accurately Identifies Men with High-grade Prostate Cancer. *Eur. Urol.* **2015**, *68*, 464–470. [CrossRef]
19. Tomlins, S.A.; Day, J.R.; Lonigro, R.J.; Hovelson, D.H.; Siddiqui, J.; Kunju, L.P.; Dunn, R.L.; Meyer, S.; Hodge, P.; Groskopf, J.; et al. Urine TMPRSS2:ERG Plus PCA3 for Individualized Prostate Cancer Risk Assessment. *Eur. Urol.* **2015**, *70*, 45–53. [CrossRef]
20. Hyvönen, M.T.; Keinänen, T.A.; Nuraeva, G.K.; Yanvarev, D.V.; Khomutov, M.; Khurs, E.N.; Kochetkov, S.N.; Vepsäläinen, J.; Zhgun, A.A.; Khomutov, A.R. Hydroxylamine analogue of agmatine: Magic bullet for arginine decarboxylase. *Biomolecules* **2020**, *10*, 406. [CrossRef]
21. Meurling, L.; Márquez, M.; Nilsson, S.; Holmberg, A.R. Polymer-conjugated guanidine is a potentially useful anti-tumor agent. *Int. J. Oncol.* **2009**, *35*, 281–285. [PubMed]
22. Keshet, R.; Erez, A. Arginine and the metabolic regulation of nitric oxide synthesis in cancer. *Dis. Model. Mech.* **2018**, *11*. [CrossRef]
23. Patil, M.; Bhaumik, J.; Babykutty, S.; Banerjee, U.C.; Fukumura, D. Arginine dependence of tumor cells: Targeting a chink in cancer's armor. *Oncogene* **2016**, *35*, 4957–4972. [CrossRef] [PubMed]
24. Al-Koussa, H.; El Mais, N.; Maalouf, H.; Abi-Habib, R.; El-Sibai, M. Arginine deprivation: A potential therapeutic for cancer cell metastasis? A review. *Cancer Cell Int.* **2020**, *20*, 1–7. [CrossRef]
25. Bronte, V.; Zanovello, P. Regulation of immune responses by L-arginine metabolism. *Nat. Rev. Immunol.* **2005**, *5*, 641–654. [CrossRef] [PubMed]
26. Sikalidis, A.K. Amino Acids and Immune Response: A Role for Cysteine, Glutamine, Phenylalanine, Tryptophan and Arginine in T-cell Function and Cancer? *Pathol. Oncol. Res.* **2015**, *21*, 9–17. [CrossRef]
27. Raber, P.; Ochoa, A.C.; Rodríguez, P.C. Metabolism of L-arginine by myeloid-derived suppressor cells in cancer: Mechanisms of T cell suppression and therapeutic perspectives. *Immunol. Investig.* **2012**, *41*, 614–634. [CrossRef]
28. Peranzoni, E.; Marigo, I.; Dolcetti, L.; Ugel, S.; Sonda, N.; Taschin, E.; Mantelli, B.; Bronte, V.; Zanovello, P. Role of arginine metabolism in immunity and immunopathology. *Immunobiology* **2008**, *212*, 795–812. [CrossRef]
29. Pereira, A.B.C. Efeitos da nutrição imunomoduladora na recuperação cirurgica de doentes com cancro gástrico. 2019. Available online: https://repositorio-aberto.up.pt/bitstream/10216/122142/2/350047.pdf (accessed on 27 January 2022).
30. García-Navas, R.; Munder, M.; Mollinedo, F. Depletion ofL-arginine induces autophagy as a cytoprotective response to endoplasmic reticulum stress in human T lymphocytes. *Autophagy* **2012**, *8*, 1557–1576. [CrossRef]
31. Miller-Fleming, L.; Olin-Sandoval, V.; Campbell, K.; Ralser, M. Remaining mysteries of Molecular Biology: The role of polyamines in the cell. *J. Mol. Biol.* **2015**, *427*, 3389–3406. [CrossRef]
32. Flynn, A.T.; Hogarty, M.D. Myc, Oncogenic Protein Translation, and the Role of Polyamines. *Med Sci.* **2018**, *6*, 41. [CrossRef] [PubMed]
33. Betts, A.M.; Waite, I.; Neal, D.E.; Robson, C.N. Androgen regulation of ornithine decarboxylase in human prostatic cells identified using differential display. *FEBS Lett.* **1997**, *405*, 328–332. [CrossRef]
34. Nilsson, J.A.; Keller, U.B.; Baudino, T.A.; Yang, C.; Norton, S.; Old, J.A.; Nilsson, L.M.; Neale, G.; Kramer, D.L.; Porter, C.W.; et al. Targeting ornithine decarboxylase in Myc-induced lymphomagenesis prevents tumor formation. *Cancer Cell* **2005**, *7*, 433–444. [CrossRef] [PubMed]
35. Synakiewicz, A.; Stachowicz-Stencel, T.; Adamkiewicz-Drozynska, E. The role of arginine and the modified arginine deiminase enzyme ADI-PEG 20 in cancer therapy with special emphasis on Phase I/II clinical trials. *Expert Opin. Investig. Drugs* **2014**, *23*, 1517–1529. [CrossRef]
36. Dillon, B.J.; Holtsberg, F.W.; Ensor, M.; Bomalaski, J.S.; Clark, M.A. Biochemical characterization of the arginine degrading enzymes arginase and arginine deiminase and their effect on nitric oxide production. *Med. Sci. Monit.* **2002**, *8*, BR248–BR253.
37. Butler, M.; van der Meer, L.T.; van Leeuwen, F.N. Amino acid depletion therapies: Starving cancer cells to death. *Trends Endocrinol. Metab.* **2021**, *32*, 367–381. [CrossRef]
38. Bostwick, D.G.; Qian, J.; Frankel, K. The incidence of high grade prostatic intraepithelial neoplasia in needle biopsies. *J. Urol.* **1995**, *154*, 1791–1794. [CrossRef]
39. Iczkowski, K.A.; MacLennan, G.T.; Bostwick, D.G. Atypical small acinar proliferation suspicious for malignancy in prostate needle biopsies: Clinical significance in 33 cases. *Am. J. Surg. Pathol.* **1997**, *21*, 1489–1495. [CrossRef]
40. Scattoni, V.; Roscigno, M.; Freschi, M.; Dehò, F.; Raber, M.; Briganti, A.; Fantini, G.; Nava, L.; Montorsi, F.; Rigatti, P. Atypical small acinar proliferation (ASAP) on extended prostatic biopsies: Predictive factors of cancer detection on repeat biopsies. *Arch. Ital. di Urol. e Androl.* **2005**, *77*, 31–36.
41. Epstein, J.I.; Herawi, M. Prostate Needle Biopsies Containing Prostatic Intraepithelial Neoplasia or Atypical Foci Suspicious for Carcinoma: Implications for Patient Care. *J. Urol.* **2006**, *175*, 820–834. [CrossRef]
42. Zhou, M.; Chinnaiyan, A.M.; Kleer, C.G.; Lucas, P.C.; Rubin, M.A. Alpha-methylacyl-coa racemase: A novel tumor marker over-expressed in several human cancers and their precursor lesions. *Am. J. Surg. Pathol.* **2002**, *26*, 926–931. [CrossRef] [PubMed]
43. Halushka, M.; Kahane, H.; Epstein, J.I. Negative 34βE12 staining in a small focus of atypical glands on prostate needle biopsy: A follow-up study of 332 cases. *Hum. Pathol.* **2004**, *35*, 43–46. [CrossRef] [PubMed]
44. Bostwick, D.G. High grade prostatic intraepithelial neoplasia. The most likely precursor of prostate cancer. *Cancer* **1995**, *75*, 1823–1836. [CrossRef]

45. Bostwick, D.G.; Brawer, M.K. Prostatic Intra-Epithelial Neoplasia and Early Invasion in Prostate Cancer. *Cancer* **1987**, *59*, 788–794. [CrossRef]
46. Gokden, N.; Roehl, K.A.; Catalona, W.J.; Humphrey, P.A. High-grade prostatic intraepithelial neoplasia in needle biopsy as risk factor for detection of adenocarcinoma: Current level of risk in screening population. *Urology* **2005**, *65*, 538–542. [CrossRef]
47. Bishara, T.; Ramnani, D.M.; Epstein, J.I. High-grade prostatic intraepithelial neoplasia on needle biopsy: Risk of cancer on repeat biopsy related to number of involved cores and morphologic pattern. *Am. J. Surg. Pathol.* **2004**, *28*, 629–633. [CrossRef]
48. Coradduzza, D.; Azara, E.; Medici, S.; Arru, C.; Solinas, T.; Madonia, M.; Zinellu, A. A preliminary study procedure for detection of polyamines in plasma samples as a potential diagnostic tool in prostate cancer. *J. Chromatogr. B* **2020**, *1162*, 122468. [CrossRef]
49. Bostwick, D.G.; Qian, J. High-grade prostatic intraepithelial neoplasia. *Mod. Pathol.* **2004**, *17*, 360–379. [CrossRef]
50. Andras, I.; Telecan, T.; Crisan, D.; Cata, E.; Kadula, P.; Andras, D.; Bungardean, M.; Coman, I.; Crisan, N. Different clinical significance of asap/hgpin pattern in systematic vs. Mri-us fusion guided prostate biopsy. *Exp. Ther. Med.* **2020**, *20*, 1. [CrossRef]
51. van Leenders, G.J.; van der Kwast, T.H.; Grignon, D.J.; Evans, A.J.; Kristiansen, G.; Kweldam, C.F.; Litjens, G.; McKenney, J.K.; Melamed, J.; Mottet, N.; et al. The 2019 International Society of Urological Pathology (ISUP) Consensus Conference on Grading of Prostatic Carcinoma. *Am. J. Surg. Pathol.* **2020**, *44*, e87–e99. [CrossRef]
52. Bylesjö, M.; Rantalainen, M.; Cloarec, O.; Nicholson, J.K.; Holmes, E.; Trygg, J. OPLS discriminant analysis: Combining the strengths of PLS-DA and SIMCA classification. *J. Chemom.* **2006**, *20*, 341–351. [CrossRef]
53. Greiner, M.; Pfeiffer, D.; Smith, R. Principles and practical application of the receiver-operating characteristic analysis for diagnostic tests. *Prev. Veter-Med.* **2000**, *45*, 23–41. [CrossRef]
54. Telesca, D.; Etzioni, R.; Gulati, R. Estimating Lead Time and Overdiagnosis Associated with PSA Screening from Prostate Cancer Incidence Trends. *Biometrics* **2007**, *64*, 10–19. [CrossRef] [PubMed]
55. Satriano, J.; Matsufuji, S.; Murakami, Y.; Lortie, M.J.; Schwartz, D.; Kelly, C.J.; Hayashi, S.-I.; Blantz, R.C. Agmatine Suppresses Proliferation by Frameshift Induction of Antizyme and Attenuation of Cellular Polyamine Levels. *J. Biol. Chem.* **1998**, *273*, 15313–15316. [CrossRef]
56. Regunathan, S.; Youngson, C.; Raasch, W.; Wang, H.; Reis, D.J. Imidazoline receptors and agmatine in blood vessels: A novel system inhibiting vascular smooth muscle proliferation. *J. Pharmacol. Exp. Ther.* **1996**, *276*, 1272–1282. [PubMed]
57. Vargiu, C.; Cabella, C.; Belliardo, S.; Cravanzola, C.; Grillo, M.A.; Colombatto, S. Agmatine modulates polyamine content in hepatocytes by inducing spermidine/spermine acetyltransferase. *Eur. J. Biochem.* **1999**, *259*, 933–938. [CrossRef] [PubMed]
58. Wang, J.-Y.; McCormack, S.; Viar, M.; Wang, H.; Tzen, C.-Y.; Scott, R.; Johnson, L. Decreased expression of protooncogenes c-fos, c-myc, and c-jun following polyamine depletion in iec-6 cells. *Am. J. Physiol. -Gastrointest. Liver Physiol.* **1993**, *265*, G331–G338. [CrossRef]
59. Li, L.; Rao, J.N.; Bass, B.L.; Wang, J.-Y. Nf-κb activation and susceptibility to apoptosis after polyamine depletion in intestinal epithelial cells. *Am. J. Physiol. -Gastrointest. Liver Physiol.* **2001**, *280*, G992–G1004. [CrossRef]
60. Stephenson, A.; Christian, J.; Seidel, E. Polyamines regulate eukaryotic initiation factor 4E-binding protein 1 gene transcription. *Biochem. Biophys. Res. Commun.* **2004**, *323*, 204–212. [CrossRef]
61. Patel, A.R.; Wang, J.Y. Polyamines modulate transcription but not posttranscription of c-myc and c-jun in IEC-6 cells. *Am. J. Physiol. Content* **1997**, *273*, C1020–C1029. [CrossRef]
62. Li, L.; Liu, L.; Rao, J.N.; Esmaili, A.; Strauch, E.D.; Bass, B.L.; Wang, J. JunD stabilization results in inhibition of normal intestinal epithelial cell growth through P21 after polyamine depletion. *Gastroenterology* **2002**, *123*, 764–779. [CrossRef] [PubMed]
63. Li, L.; Li, J.; Rao, J.N.; Li, M.; Bass, B.L.; Wang, J.-Y. Inhibition of polyamine synthesis induces p53 gene expression but not apoptosis. *Am. J. Physiol. Content* **1999**, *276*, C946–C954. [CrossRef] [PubMed]
64. Rowe, W.A.; Blackmon, D.L.; Montrose, M.H. Propionate activates multiple ion transport mechanisms in the HT29-18-C1 human colon cell line. *Am. J. Physiol. Content* **1993**, *265*, G564–G571. [CrossRef] [PubMed]
65. Kapancık, S.; Çelik, V.; Kılıçkap, S.; Kacan, T.; Kapancik, S. The relationship of agmatine deficiency with the lung cancer. *Uhod-Uluslararasi Hematoloji-Onkoloji Dergisi* **2016**, *26*. [CrossRef]
66. Albaugh, V.L.; Pinzon-Guzman, C.; Barbul, A. Arginine metabolism and cancer. *J. Surg. Oncol.* **2017**, *115*, 273. [CrossRef]
67. Raasch, W.; Schäfer, U.; Chun, J.; Dominiak, P. Biological significance of agmatine, an endogenous ligand at imidazoline binding sites. *J. Cereb. Blood Flow Metab.* **2001**, *133*, 755–780. [CrossRef]
68. Satriano, J.; Isome, M.; Casero, R.A.; Thomson, S.C.; Blantz, R.C. Polyamine transport system mediates agmatine transport in mammalian cells. *Am. J. Physiol. Physiol.* **2001**, *281*, C329–C334. [CrossRef]
69. Choi, Y.S.; Cho, Y.D. Effects of agmatine on polyamine metabolism and the growth of prostate tumor cells. *BMB Rep.* **1999**, *32*, 173–180.
70. Molderings, G.J.; Kribben, B.; Heinen, A.; Schröder, D.; Brüss, M.; Göthert, M. Intestinal tumor and agmatine (decarboxylated arginine) low content in colon carcinoma tissue specimens and inhibitory effect on tumor cell proliferation in vitro. *Cancer* **2004**, *101*, 858–868. [CrossRef]
71. Wang, J.-F.; Su, R.-B.; Wu, N.; Xu, B.; Lu, X.-Q.; Liu, Y.; Li, J. Inhibitory effect of agmatine on proliferation of tumor cells by modulation of polyamine metabolism. *Acta Pharmacol. Sin.* **2005**, *26*, 616–622.